

# Final state interactions in the $D_s^+ \rightarrow \omega \pi^+$ and $D_s^+ \rightarrow \rho^0 \pi^+$ decays

S. Fajfer,<sup>1,2</sup> A. Prapotnik,<sup>2</sup> P. Singer,<sup>3</sup> and J. Zupan<sup>2,3</sup>

<sup>1</sup>*Department of Physics, University of Ljubljana, Jadranska 19, 1000 Ljubljana, Slovenia*

<sup>2</sup>*J. Stefan Institute, Jamova 39, P. O. Box 300, 1001 Ljubljana, Slovenia*

<sup>3</sup>*Department of Physics, Technion-Israel Institute of Technology, Haifa 32000, Israel*

(Received 8 August 2003; published 14 November 2003)

We investigate the decay mechanisms in the  $D_s^+ \rightarrow \omega \pi^+$  and  $D_s^+ \rightarrow \rho^0 \pi^+$  transitions. The naive factorization ansatz predicts a vanishing amplitude for the  $D_s^+ \rightarrow \omega \pi^+$  decay, while the  $D_s^+ \rightarrow \rho^0 \pi^+$  decay amplitude does have an annihilation contribution also in this limit. Both decays can proceed through intermediate states of hidden strangeness, e.g.  $K, K^*$ , which we estimate in this paper. These contributions can explain the experimental value for the  $D_s^+ \rightarrow \omega \pi^+$  decay rate, which no longer can be viewed as a clean signature of the annihilation decay of  $D_s^+$ . The combination of the  $\pi(1300)$  pole dominated annihilation contribution and the internal  $K, K^*$  exchange can saturate the present experimental upper bound on the  $D_s^+ \rightarrow \rho^0 \pi^+$  decay rate, which is therefore expected to be within experimental reach. Finally, the proposed mechanism of hidden strangeness final state interactions constitutes only a small correction to the Cabibbo allowed decay rates  $D_s \rightarrow KK^*, \phi \pi$ , which are well described already in the factorization approximation.

DOI: 10.1103/PhysRevD.68.094012

PACS number(s): 13.25.Ft, 12.15.Ji

## I. INTRODUCTION

It has been suggested [1] that the observation of the  $D_s^+ \rightarrow \omega \pi^+$  decay

$$BR(D_s^+ \rightarrow \omega \pi^+) = (2.8 \pm 1.1) \times 10^{-3} \quad (1)$$

can be seen as a clean signature of the annihilation decay of  $D_s^+$ . The sizes of these contributions are of great phenomenological interest, but are very hard to obtain from theoretical considerations. In particular, the factorization approximation gives a vanishing prediction for  $BR(D_s^+ \rightarrow \omega \pi^+)$ , as an immediate consequence of the fact that, due to the isospin and  $G$  parity  $I^G = 1^+$  of the  $\omega \pi^+$  state, there are no annihilation contributions with one intermediate resonant state (cf. also Fig. 1). The interpretation of branching ratio (1) as an (almost) purely annihilation decay would then also give important information about the otherwise relatively poorly known sizes of annihilation diagrams in other related hadronic decays. In this paper, however, we will argue that the experimental value for the  $D_s^+ \rightarrow \omega \pi^+$  transition can be accommodated (already) by considering *only* the color suppressed spectator decay with subsequent final state interactions (FSI). This leaves little room for unambiguous study of annihilation effects from the  $\omega \pi^+$  decay mode.

Another issue that we address is the size of the  $D_s^+ \rightarrow \rho^0 \pi^+$  transition. The experimental situation regarding this decay is somewhat unclear. The difficulties arise from the fact that the  $D_s^+ \rightarrow \rho^0 \pi^+$  decay is observed as a resonance in the three body decay  $D_s^+ \rightarrow \pi^- \pi^+ \pi^+$ , which is dominated by the decays through isoscalar resonances,  $f_0(980) \pi^+$ ,  $f_0(1370) \pi^+$  [2,3]. The decay  $D_s^+ \rightarrow \rho^0 \pi^+$  therefore constitutes just a small correction to these dominant processes. The two available experimental analyses give

$$BR(D_s^+ \rightarrow \rho^0 \pi^+) < 7 \times 10^{-4} \quad (2)$$

from [2], and

$$BR(D_s^+ \rightarrow \rho^0 \pi^+) = (5.9 \pm 4.6) \times 10^{-4} \quad (3)$$

from [3], where the first is a 90% C.L. limit, while in the second case we have added all the errors in quadrature. Clearly, the two measurements are in agreement with each other. The error on the number from [3] is still very large and can at best be viewed as an indication toward possible values for  $BR(D_s^+ \rightarrow \rho^0 \pi^+)$ . In particular, it is still compatible with zero. As we will show in the following, however, the expectations for  $BR(D_s^+ \rightarrow \rho^0 \pi^+)$  one gets from spectator decays with FSI and/or annihilation diagrams are just in the same ballpark as the above experimental indications.

An important difference between  $D_s^+ \rightarrow \omega \pi^+$  and  $D_s^+ \rightarrow \rho^0 \pi^+$  transitions are the quantum numbers of the final state. The  $(\omega \pi^+)$  is a  $I^G(J^P) = 1^+(0^-)$  state, while the  $(\rho^0 \pi^+)$  can be either in the  $I^G = 1^-$  or  $2^-$  state, again with  $J^P = 0^-$ . A scan through the Particle Data Group (PDG) book [4] reveals that there are no resonant states with an  $I^G(J^P) = 1^+(0^-)$  assignment, while there are three known states with  $I^G(J^P) = 1^-(0^-)$ , the two strongly decaying resonances  $\pi(1300)$  and  $\pi(1800)$ , and the pion.

The presence of resonances near the  $D_s$  meson mass with the quantum numbers of the  $(\rho^0 \pi^+)$  state indicates an enhancement of annihilation contributions, which in this case can proceed through an intermediate resonating state (see

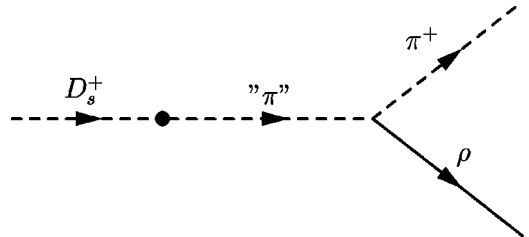


FIG. 1. Annihilation diagram of  $D_s^+ \rightarrow \rho^0 \pi^+$  decay with “ $\pi^+$ ” =  $\pi, \pi(1300), \pi(1800)$ , with the dot representing the weak vertex.

Fig. 1). To gain an insight on the numerical importance of the annihilation processes we estimate the contribution coming from the  $\pi(1300)$  intermediate state. To do so, we need to estimate the decay constant of  $\pi(1300)$ . Taking the PDG [4] upper bound for  $\tau \rightarrow \pi(1300) \nu_\tau$  one arrives at  $f_{\pi(1300)} < 4$  MeV. In the factorization approximation for the weak vertex (for more details see Sec. II) we then get

$$BR(D_s^+ \rightarrow \rho^0 \pi^+)_{\pi(1300)} < 7 \times 10^{-4}, \quad (4)$$

where we have used  $f_{D_s} = 230$  MeV, together with the conservative assumptions of  $BR(\pi(1300) \rightarrow \rho \pi) \sim 100\%$  and  $\Gamma(\pi(1300))$  equal to its upper experimental bound of 600 MeV. Most probably this slightly overestimates the contribution of the  $\pi(1300)$  intermediate resonant state to the  $D_s^+ \rightarrow \rho^0 \pi^+$  decay width, as also the presence (but not the size) of other decay channels of  $\pi(1300)$  has been seen experimentally [e.g.  $\pi(1300) \rightarrow (\pi\pi)_{S\text{-wave}} \pi$  [4]]. Note in particular that the above assumptions about the  $\pi(1300) \rightarrow \rho \pi$  decay width correspond to the case where  $g_{\rho\pi\pi(1300)} \approx g_{\rho\pi\pi}$ . We therefore do not expect the  $\pi(1300)$  contribution to  $BR(D_s^+ \rightarrow \rho^0 \pi^+)$  to lie significantly below the upper limit (4).

The importance of the upper limit (4) is that the contribution from  $\pi(1300)$  can even saturate the 90% C.L. experimental upper bound (2). Of course the actual size of the  $\pi(1300)$  contribution is not known and lies somewhere below the upper bound (4). Also, interference with other annihilation contributions from intermediate  $\pi$  and  $\pi(1800)$  states can somewhat change the above estimate [using partially conserved axial current (PCAC), the contribution from  $\pi$  was found in [5] to be negligible, while the contribution of  $\pi(1800)$  is difficult to estimate due to the lack of experimental data]. Furthermore, as we will show in the next section, the contributions of final state interactions fall in exactly the same range [cf. Eq. (15)]. The lesson to be learned from this simple exercise is that, unless there are large cancellations, the value of  $BR(D_s^+ \rightarrow \rho^0 \pi^+)$  is expected to be near to its present experimental upper bound and should be measured by the FOCUS Collaboration in the near future [6].

On the other hand note that, as explained above, *no such resonance enhancements* of annihilation contributions are possible for the  $(\omega \pi^+)$  final state. How can then one explain a relatively large experimental value for  $BR(D_s^+ \rightarrow \omega \pi^+)$ , Eq. (1)? The answer lies in the fact that there are multibody intermediate states that do have correct values of  $I^G$  and  $J^P$ , for instance the two-body  $(K^{(*)} \bar{K}^{(*)})$  states (see Fig. 2). Moreover, such states of *hidden strangeness* can be obtained from a (color suppressed) spectator decay of the  $D_s^+$  meson and are therefore expected to be sizable. We will estimate the sizes of these contributions in the next section.

## II. HIDDEN STRANGENESS FSI

In estimating the contributions from hidden strangeness intermediate states that can arise from spectator quark diagrams, we will resort to the following simplifications:

- (i) Only two-body intermediate states with  $s, \bar{s}$  quantum

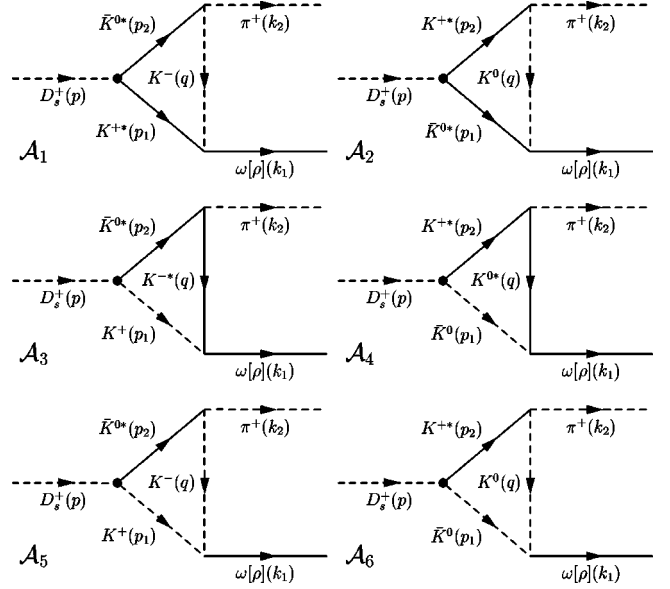


FIG. 2. The  $K, K^*$  meson contributions in the  $D_s^+ \rightarrow \omega \pi^+$  and  $D_s^+ \rightarrow \rho^0 \pi^+$  decay amplitudes.

numbers will be taken into account. Moreover, only the contributions of lowest lying pseudoscalar and vector states (neglecting their decay widths) will be considered. Note that the rescattering through intermediate  $K, K^*$  states is possible for both  $\rho^0 \pi^+$  as well as  $\omega \pi^+$  final state (cf. Fig. 2), while the rescattering with intermediate  $\eta$  or  $\eta'$  is possible only in the case of the  $\omega \pi^+$  final state due to isospin and  $G$  parity conservation (cf. Fig. 3).

(ii) For the weak transition  $D_s^+ \rightarrow (K^{(*)} \bar{K}^{(*)})^+$  in the  $D_s^+ \rightarrow (K^{(*)} \bar{K}^{(*)})^+ \rightarrow \rho^0 \pi^+$  and  $D_s^+ \rightarrow (K^{(*)} \bar{K}^{(*)})^+ \rightarrow \omega \pi^+$  decay chains as well as for the weak transition  $D_s^+ \rightarrow \eta(\eta') \rho^+$  in the  $D_s^+ \rightarrow \eta(\eta') \rho^+ \rightarrow \omega \pi^+$  decay chain we will use the factorization approximation. The weak Lagrangian is therefore

$$\mathcal{L}_{\text{weak}} = -\frac{G_f}{\sqrt{2}} V_{cs} V_{ud}^* [a_1 (\bar{u}d)_H (\bar{s}c)_H + a_2 (\bar{s}d)_H (\bar{u}c)_H], \quad (5)$$

with  $(\bar{u}d)_H, \dots$  the hadronized  $V-A$  weak currents,  $V_{ij}$  the Cabibbo-Kobayashi-Maskawa (CKM) matrix elements, and  $a_{1,2}$  the effective (phenomenological) Wilson coefficients taken to be  $a_1 = 1.26$  and  $a_2 = -0.52$  [7–9].

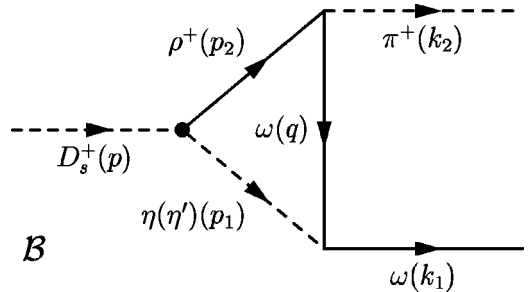


FIG. 3. The intermediate  $\eta, \eta', \rho^+$  contributions in the  $D_s^+ \rightarrow \omega \pi^+$  decay.

TABLE I. Form factors at  $q^2=0$  [15]. The results in the first five columns are for  $D_s \rightarrow K, K^* l \nu_l$  transitions. The last column stands for the form factor appearing in  $D_s \rightarrow \eta_s l \nu_l$  (the  $s\bar{s}$  component of  $\eta, \eta'$ ) transition.

Form factor	$F_+$	$V$	$A_0$	$A_1$	$A_2$	$F_{\eta_s,+}$
$f(0)$	0.72	1.04	0.67	0.57	0.42	0.78
$\sigma$	0.2	0.24	0.2	0.29	0.58	0.23

(iii) Finally, the strong interactions are taken into account through the following effective Lagrangian [10–12]:

$$\mathcal{L}_{\text{strong}} = \frac{ig_{\rho\pi\pi}}{\sqrt{2}} \text{Tr}(\rho^\mu [\Pi, \partial_\mu \Pi]) - 4 \frac{C_{V\Pi\Pi}}{f} \epsilon^{\mu\nu\alpha\beta} \text{Tr}(\partial_\mu \rho_\nu \partial_\alpha \rho_\beta \Pi), \quad (6)$$

where  $\Pi$  and  $\rho^\mu$  are  $3 \times 3$  matrices containing pseudoscalar and vector meson operators, respectively, and  $f$  is a pseudo-scalar decay constant (11). We use numerical values (see [10–12])  $C_{V\Pi\Pi} = 0.33$ , and  $g_{\rho\pi\pi} = 5.9$ .

We have checked that the use of factorization [at tree level, with values of form factors as given below in Eqs. (7)–(11) and in Table I] for the  $D_s^+ \rightarrow K^{*+} \bar{K}^{*0}$ ,  $D_s^+ \rightarrow K^+ \bar{K}^{*0}$  and  $D_s^+ \rightarrow \bar{K}^0 K^{*+}$  decays gives reasonable estimates of the measured rates (note that we do not need  $D_s^+ \rightarrow \bar{K}^0 K^+$  in further considerations), with the results listed in Table II. In these results the annihilation contributions have been neglected since they are an order of magnitude smaller. We also neglect the triangle graphs of the sort shown on Figs. 2, 3 as we expect them (based on the numerical results for  $\omega \pi^+$ ,  $\rho^0 \pi^+$ ) to be suppressed relative to the tree level contributions.

The situation in the case of  $\eta, \eta'$  intermediate states is not so favorable. To treat the  $\eta, \eta'$  mixing we use the approach of Ref. [13] with the value of the mixing angle transforming between  $\eta, \eta'$  and  $\eta_q \sim (u\bar{u} + d\bar{d})/\sqrt{2}$ ,  $\eta_s \sim s\bar{s}$  states taken to be  $\phi = 40^\circ$ . The factorization approach then gives a reasonable description of  $D_s^+ \rightarrow \rho^+ \eta$  decay, while it does not reproduce satisfactorily the experimental result for  $D_s^+ \rightarrow \rho^+ \eta'$  (cf. Table II). This is a known problem as the  $D_s^+ \rightarrow \rho^+ \eta'$

TABLE II. The branching ratios for the  $D_s^+$  two-body decays: in the second column the experimental results are listed, while in the third the predictions are given when the factorization approximation is used.

Decay	$BR_{\text{exp}}$	$BR_{\text{th}}$
$D_s^+ \rightarrow K^{*+} \bar{K}^{*0}$	$(5.8 \pm 2.5)\%$	6.4%
$D_s^+ \rightarrow K^+ \bar{K}^{*0}$	$(3.3 \pm 0.9)\%$	3.4%
$D_s^+ \rightarrow K^{*+} \bar{K}^0$	$(4.3 \pm 1.4)\%$	2.7%
$D_s^+ \rightarrow \eta \rho^+$	$(10.8 \pm 3.1)\%$	5.6%
$D_s^+ \rightarrow \eta' \rho^+$	$(10.1 \pm 2.8)\%$	2.2%

rate is very difficult to reproduce by any of the present approaches [8,9,14]. This inevitably introduces some further uncertainty into our approach, yet the resulting uncertainty is not expected to affect significantly our main conclusions.

For the weak current matrix elements between  $D_s^+$  and vector or pseudoscalar final states we use a common decomposition

$$\begin{aligned} \langle V(k) | \bar{q} \Gamma^\mu q | D_s(p) \rangle &= \epsilon^{\mu\nu\alpha\beta} \epsilon_\nu p_\alpha k_\beta \frac{2V(q^2)}{M_p + m_V} \\ &+ 2im_V \frac{\epsilon \cdot q}{q^2} q^\mu A_0(q^2) + i(M + m_V) \\ &\times \left[ \epsilon^\mu - \frac{\epsilon \cdot q}{q^2} q^\mu \right] A_1(q^2) - i \frac{\epsilon \cdot q}{M + m_V} \\ &\times \left[ P^\mu - \frac{M^2 - m_V^2}{q^2} q^\mu \right] A_2(q^2), \quad (7) \end{aligned}$$

$$\begin{aligned} \langle P(k) | \bar{q} \Gamma^\mu q | D_s(p) \rangle &= \left( P^\mu - \frac{(M^2 - m^2)}{q^2} q^\mu \right) F_+(q^2) \\ &+ \frac{(M^2 - m^2)}{q^2} q^\mu F_0(q^2), \quad (8) \end{aligned}$$

where  $V$  is a vector meson characterized by the polarization vector  $\epsilon^\mu$  and mass  $m_V$ , while pseudoscalar mesons  $P, D_s$  have masses  $m, M$ . We use further abbreviations  $\Gamma^\mu = \gamma^\mu (1 - \gamma^5)$ ,  $q^\mu = p^\mu - k^\mu$ , and  $P^\mu = p^\mu + k^\mu$ .

For the  $q^2$  dependence of the form factors we use results of [15], based on a quark model calculation combined with a fit to lattice and experimental data. Reference [15] provides a simple fit to their numerical results with the form factors  $F_+(q^2)$ ,  $V(q^2)$ , and  $A_0(q^2)$  described by double pole  $q^2$  dependence

$$f(q^2) = \frac{f(0)}{(1 - q^2/M^2)(1 - \sigma q^2/M^2)}, \quad (9)$$

while single pole parametrization

$$f(q^2) = \frac{f(0)}{(1 - \sigma q^2/M^2)} \quad (10)$$

can be used for  $A_{1,2}(q^2)$ , as the contributing resonance lies farther away from the physical region (note that this parametrization applies also to the  $F_0$  form factor which, however, does not contribute in the processes we discuss in this paper). The values of  $f(0)$  and  $\sigma$  are listed in Table I and are taken from [15]. We use  $M = 1.97$  GeV in the expression for  $A_0$ , while  $M = 2.11$  GeV is used for other form factors [15]. Incidentally, the parametrizations of form factors (9), (10) make all the loop diagrams in Figs. 2 and 3 finite, so that no regularization procedure is needed [we have also checked that the numerical results do not change significantly if one uses a single pole parametrization instead of Eq. (9) and then

TABLE III. The dispersive  $\mathcal{A}_{iD}$  and absorptive  $\mathcal{A}_{iA}$  parts of the amplitudes (in units of  $10^{-3}$  GeV) for the  $D_s^+ \rightarrow \omega \pi^+$  decay corresponding to the diagrams on Fig. 2 ( $\mathcal{A}_i$ ) and Fig. 3 ( $\mathcal{B}_{\eta, \eta'}$ ). The amplitudes for the  $D_s^+ \rightarrow \rho^0 \pi^+$  decay (neglecting the mass difference between  $m_\rho$  and  $m_\omega$ ) are obtained by inverting the sign of  $\mathcal{A}_{iD}, \mathcal{A}_{iA}$  for even  $i$ , while  $\mathcal{B}_{\eta, \eta'} = 0$ .

$D_s^+ \rightarrow \omega \pi^+$	$\mathcal{A}_1$	$\mathcal{A}_2$	$\mathcal{A}_3$	$\mathcal{A}_4$	$\mathcal{A}_5$	$\mathcal{A}_6$	$\mathcal{B}_\eta$	$\mathcal{B}_{\eta'}$
$\mathcal{A}_{iD}$	-0.7	0.7	-1.1	-1.4	11.3	12.5	1.3	3.6
$\mathcal{A}_{iA}$	-0.7	0.7	3.3	1.5	-4.0	-19.7	-7.2	-3.7

uses a cut-off regularization with some scale above but close enough to the  $D_s$  meson mass].

For the decay constants, defined through

$$\langle 0 | \bar{q} \gamma^\mu \gamma_5 q | P(p) \rangle = i f_P p^\mu, \quad \langle 0 | \bar{q} \gamma^\mu q | V(p) \rangle = g_V \varepsilon^\mu, \quad (11)$$

we use the following values:  $f_D = 0.207$  GeV and  $f_{D_s} = 1.13 f_D$  as obtained on the lattice [16] and for the rest  $f_K = 0.16$  GeV,  $|g_K^*| = 0.19$  GeV<sup>2</sup>,  $|g_\rho| = 0.17$  GeV<sup>2</sup>, and  $|g_\omega| = 0.15$  GeV<sup>2</sup> coming from the experimental measurements [4].

The amplitudes for the  $D_s^+ \rightarrow \omega \pi^+$  and  $D_s^+ \rightarrow \rho^0 \pi^+$  decays can be written as

$$\mathcal{A}(D_s^+(p) \rightarrow \omega(\varepsilon, k_1) \pi^+(k_2)) = \frac{G_f}{\sqrt{2}} \varepsilon \cdot k_2 \left( \sum_i \mathcal{A}_i^{(\omega)} + \mathcal{B} \right), \quad (12)$$

$$\mathcal{A}(D_s^+(p) \rightarrow \rho^0(\varepsilon, k_1) \pi^+(k_2)) = \frac{G_f}{\sqrt{2}} \varepsilon \cdot k_2 \sum_i \mathcal{A}_i^{(\rho)}, \quad (13)$$

with  $\varepsilon$  the helicity zero polarization vector of the  $\omega$  or  $\rho^0$  vector mesons, while  $k_2$  is the pion momentum. The reduced amplitudes  $\mathcal{A}_i^{(\rho),(\omega)}$  and  $\mathcal{B}$  correspond to the diagrams on Figs. 2 and 3, respectively [note that in our phase convention for Clebsch-Gordan coefficients  $\mathcal{A}_i^{(\rho)} = (-1)^{i+1} \mathcal{A}_i^{(\omega)}$ , i.e. the even diagrams for the two channels on Fig. 2 differ by a sign]. The explicit expressions can be found in the Appendix. The numerical values for  $\mathcal{A}_i^{(\rho),(\omega)}$  and  $\mathcal{B}$  are given in Table III.

Combining the above results we arrive at the prediction

$$BR(D_s^+ \rightarrow \omega \pi^+) = 3.0 \times 10^{-3}. \quad (14)$$

Note that in this calculation we have used the factorization approximation for the diagram of Fig. 3, which as stated above, does not work well for the  $D_s^+ \rightarrow \rho^+ \eta, \eta'$  transition.<sup>1</sup> If one instead uses experimental input to rescale the corresponding amplitudes one ends up with  $BR(D_s^+ \rightarrow \omega \pi^+) = 4.4 \times 10^{-3}$ . We see that it is actually very easy to explain

<sup>1</sup>Adding hidden strangeness FSI in the spirit of this paper to the  $D_s^+ \rightarrow \rho^+ \eta'$  channel does not mend the discrepancy, as it gives an order of magnitude smaller contribution.

the experimental result (1) *entirely* in terms of the spectator quark transition together with FSI. The claim that  $D_s^+ \rightarrow \omega \pi^+$  can be used as a probe of annihilation contributions in hadronic physics is therefore not justified.

As what concerns the  $D_s^+ \rightarrow \rho^0 \pi^+$  transition, the FSI contributions alone give

$$BR(D_s^+ \rightarrow \rho^0 \pi^+)_{\text{FSI}} = 0.7 \times 10^{-3}, \quad (15)$$

which is almost exactly the same as our estimate of the upper bound on the annihilation contribution (4) and actually coincides with the present 90% C.L. upper bound. If there is no destructive interference between these two contributions and the contributions of FSI through higher resonances that we did not take into account, this decay mode should be established in the near future. This expectation is supported also by other theoretical approaches which give the rate for  $D_s^+ \rightarrow \rho^0 \pi^+$  to be equal [9] or even larger than the rate for  $D_s^+ \rightarrow \omega \pi^+$  decay [14,17].

The possible cancellation that *may* occur, however, make the theoretical predictions rather uncertain. Adding the FSI contribution and the maximal annihilation contributions (4) with alternating signs gives a fairly large interval

$$BR(D_s^+ \rightarrow \rho^0 \pi^+) = (0.05 - 3.5) \times 10^{-3}. \quad (16)$$

We note that the experimental uncertainties translating in the input parameters can change the values for  $BR(D_s^+ \rightarrow \rho^0 \pi^+)$  and  $BR(D_s^+ \rightarrow \omega \pi^+)$  by about 20%.

Finally, we mention that the kind of FSI contributions we were considering in this paper will not be the leading contribution in the  $D_s^+ \rightarrow \phi \pi^+$  transition, namely, this decay can proceed through the spectator quark transition directly. The use of a factorization approximation for the weak vertex leads to a prediction  $BR(D_s^+ \rightarrow \phi \pi^+) = 4.0\%$ , which is already in excellent agreement with the experimental result of  $3.6 \pm 0.9\%$ . Inclusion of FSI reduces the theoretical prediction from 4% to  $\sim 3.6\%$  and does not spoil the agreement with the experiment (it actually even improves it). The size of the shift also indicates that FSI of the type described in the present paper are in the case of  $D_s^+ \rightarrow \phi \pi^+$  transition a second order effect. Note as well that the size of the FSI correction is in agreement with the predictions for  $BR(D_s^+ \rightarrow \rho^0 \pi^+)$  and  $BR(D_s^+ \rightarrow \omega \pi^+)$ , which are an order of magnitude smaller than  $BR(D_s^+ \rightarrow \phi \pi^+)$ .

In conclusion, we found that the hidden strangeness final state interactions are very important in understanding the  $D_s^+ \rightarrow \omega \pi^+$  and  $D_s^+ \rightarrow \rho^0 \pi^+$  decay mechanism. The  $D_s^+ \rightarrow \omega \pi^+$  amplitude can be explained fully by this mechanism. As for the  $D_s^+ \rightarrow \rho^0 \pi^+$  amplitude the predictions we obtain lie in a fairly large range due to possible cancellation between FSI and single pole contributions. There is a hope that  $D_s^+ \rightarrow \rho^0 \pi^+$  will be measured soon, hopefully shedding more light on our understanding of the  $D_s^+ \rightarrow \rho^0 \pi^+$  decay



mechanism. Finally, we note that the hidden strangeness FSI discussed in this paper represents a second order effect, the inclusion of which does not spoil the good agreement of factorization approximation obtained for  $D_s \rightarrow \phi \pi, KK^*$ .

### ACKNOWLEDGMENTS

S.F., A.P., and J.Z. are supported in part by the Ministry of Education, Science and Sport of the Republic of Slovenia.

### APPENDIX: DECAY AMPLITUDES

In this appendix we list expressions for the reduced amplitudes  $\mathcal{A}_i$  and  $\mathcal{B}$  defined through Eqs. (12) and (13) and Figs. 2 and 3. We present explicitly the  $\mathcal{A}_i^{(\omega)}$  reduced amplitudes only for the  $D_s^+ \rightarrow \omega \pi^+$  decay. The corresponding expressions  $\mathcal{A}_i^{(\rho)}$  for the  $D_s^+ \rightarrow \rho^0 \pi^+$  decay are then obtained by inverting the signs of  $\mathcal{A}_i^{(\omega)}$  for even  $i$ :

$$\begin{aligned} \varepsilon \cdot k_2 \mathcal{A}_1^{(\omega)} = & \int \frac{d^4 q}{(2\pi)^4} a_2 g_K \frac{2}{m_* + M} \frac{V(0)}{1 - p_2^2/M_F^2} \epsilon_{\mu\nu\alpha\beta} p_2^\alpha p_1^\beta \frac{-i(g^{\mu\mu'} - p_2^\mu p_2^{\mu'}/m_*^2)}{p_2^2 - m_*^2} \frac{-i(g^{\nu\nu'} - p_1^\nu p_1^{\nu'}/m_*^2)}{p_1^2 - m_*^2} \frac{i}{q^2 - m^2} \frac{ig_{\rho\pi\pi}}{\sqrt{2}} \\ & \times (k_2 - q)_\mu \frac{i4C_{VV\Pi} \epsilon_{\nu'\sigma\tau\delta} p_1^\sigma \varepsilon^\tau k_1^\delta}{f_K \sqrt{2}}, \end{aligned} \quad (A1)$$

$$\begin{aligned} \varepsilon \cdot k_2 \mathcal{A}_2^{(\omega)} = & \int \frac{d^4 q}{(2\pi)^4} a_2 g_K \frac{2}{m_* + M} \frac{V(0)}{1 - p_1^2/M_F^2} \epsilon_{\mu\nu\alpha\beta} p_2^\alpha p_1^\beta \frac{-i(g^{\mu\mu'} - p_2^\mu p_2^{\mu'}/m_*^2)}{p_2^2 - m_*^2} \frac{-i(g^{\nu\nu'} - p_1^\nu p_1^{\nu'}/m_*^2)}{p_1^2 - m_*^2} \frac{i}{q^2 - m^2} \frac{ig_{\rho\pi\pi}}{\sqrt{2}} \\ & \times (q - k_2)_\mu \frac{i4C_{VV\Pi} \epsilon_{\nu'\sigma\tau\delta} p_1^\sigma \varepsilon^\tau k_1^\delta}{f_K \sqrt{2}}, \end{aligned} \quad (A2)$$

$$\begin{aligned} \varepsilon \cdot k_2 \mathcal{A}_3^{(\omega)} = & \int \frac{d^4 q}{(2\pi)^4} a_2 g_K \frac{F_+(0)}{1 - p_2^2/M_F^2} (p + p_1)_\mu \frac{-i(g^{\mu\mu'} - p_2^\mu p_2^{\mu'}/m_*^2)}{p_2^2 - m_*^2} \frac{i}{p_1^2 - m^2} \frac{-i(g^{\nu\nu'} - q^\nu q^{\nu'}/m_*^2)}{q^2 - m_*^2} \\ & \times \frac{i4C_{VV\Pi} \epsilon_{\mu'\alpha\nu'\beta} p_2^\alpha q^\beta}{f_\pi} \frac{i4C_{VV\Pi} \epsilon_{\nu\sigma\tau\delta} q^\sigma \varepsilon^\tau k_1^\delta}{f_K \sqrt{2}}, \end{aligned} \quad (A3)$$

$$\begin{aligned} \varepsilon \cdot k_2 \mathcal{A}_4^{(\omega)} = & \int \frac{d^4 q}{(2\pi)^4} a_2 \left[ 2im_* \frac{p_{1\mu} p_1^\lambda}{p_1^2} \frac{A_0(0)}{1 - p_1^2/M_A^2} - i \frac{p_{1\mu}}{M + m_*} \frac{A_2(0)}{1 - p_1^2/M_F^2} \left( (p + p_2)^\lambda - \frac{M^2 - m_*^2}{p_1^2} p_1^\lambda \right) \right] \\ & \times (-if_K p_1)_\lambda \frac{i}{p_1^2 - m^2} \frac{-i(g^{\mu\mu'} - p_2^\mu p_2^{\mu'}/m_*^2)}{p_2^2 - m_*^2} \frac{-i(g^{\nu\nu'} - q^\nu q^{\nu'}/m_*^2)}{q^2 - m_*^2} \frac{i4C_{VV\Pi} \epsilon_{\mu'\alpha\nu'\beta} p_2^\alpha q^\beta}{f_\pi} \\ & \times \frac{i4C_{VV\Pi} \epsilon_{\nu\sigma\tau\delta} q^\sigma \varepsilon^\tau k_1^\delta}{\sqrt{2} f_K}, \end{aligned} \quad (A4)$$

$$\begin{aligned} \varepsilon \cdot k_2 \mathcal{A}_5^{(\omega)} = & \int \frac{d^4 q}{(2\pi)^4} a_2 g_K \frac{F_+(0)}{1 - p_2^2/M_F^2} (p + p_1)_\mu \frac{-i(g^{\mu\nu} - p_2^\mu p_2^\nu/m_*^2)}{p_2^2 - m_*^2} \frac{i}{p_1^2 - m^2} \frac{i}{q^2 - m^2} \frac{ig_{\rho\pi\pi}(k_2 - q)_\nu}{\sqrt{2}} \frac{ig_{\rho\pi\pi}(q - p_1) \cdot \varepsilon}{2}, \end{aligned} \quad (A5)$$

$$\begin{aligned} \varepsilon \cdot k_2 \mathcal{A}_6^{(\omega)} = & \int \frac{d^4 q}{(2\pi)^4} a_2 \left[ 2im_* \frac{p_{1\mu} p_1^\lambda}{p_1^2} \frac{A_0(0)}{1 - p_1^2/M_A^2} - i \frac{p_{1\mu}}{M + m_*} \frac{A_2(0)}{1 - p_1^2/M_F^2} \left( (p + p_2)^\lambda - \frac{M^2 - m_*^2}{p_1^2} p_1^\lambda \right) \right] \\ & \times (-if_K p_1)_\lambda \frac{-i(g^{\mu\mu'} - p_2^\mu p_2^{\mu'}/m_*^2)}{p_2^2 - m_*^2} \frac{i}{p_1^2 - m^2} \frac{i}{q^2 - m^2} \frac{ig_{\rho\pi\pi}(q - k_2)_\nu}{\sqrt{2}} \frac{ig_{\rho\pi\pi}(q - p_1) \cdot \varepsilon}{2\sqrt{2}}. \end{aligned} \quad (A6)$$

In the expressions above we used  $m, m_*, M$  for the  $K, K^*, D_s$  mass, respectively. The pole masses used in the form factors are  $M_F = 2.11$  GeV and  $M_A = 1.97$  GeV. The definitions of momenta  $k_{1,2}$ ,  $p_{1,2}$ , and  $q$  are the same as the ones used on Figs. 2 and 3.

The  $\mathcal{B}$  part of the  $D_s^+ \rightarrow \omega \pi^+$  amplitude (Fig. 3) is

$$\begin{aligned} \varepsilon \cdot k_2 \mathcal{B} = & \int \frac{d^4 q}{(2\pi)^4} a_{1g\rho} \frac{F_{+, \eta^{(\prime)}}(0)}{1 - p_2^2/M_F^2} (p + p_1)_\mu \\ & \times \frac{-i(g^{\mu\mu'} - p_2^\mu p_2^{\mu'})}{p_2^2 - m_\rho^2} \frac{i}{p_1^2 - m_{\eta^{(\prime)}}^2} \\ & \times \frac{-i(g^{\nu\nu'} - q^\nu q^{\nu'}/m_\omega^2)}{q^2 - m_\omega^2} \frac{4i}{f_\pi} \sqrt{2} C_{V\Pi} \epsilon_{\mu'\alpha\nu'\beta} p_2^\alpha q^\beta \\ & \times \frac{4i}{f_{\eta^{(\prime)}}} K_{\eta^{(\prime)}} C_{V\Pi} \epsilon_{\nu\sigma\tau} q^\sigma \varepsilon^\tau k_1^\delta, \end{aligned} \quad (A7)$$

while  $\mathcal{B}=0$  for  $D_s^+ \rightarrow \rho^0 \pi^+$ . In Eq. (A7) we used the abbreviations

$$K_\eta = \cos \phi / \sqrt{2}, \quad K_{\eta'} = \sin \phi / \sqrt{2} \quad (A8)$$

and

$$F_{+, \eta}(0) = \sin \phi F_{\eta_s, +}(0), \quad F_{+, \eta'}(0) = \cos \phi F_{\eta_s, +}(0).$$

Finally, the decay rate for the  $D_s^+ \rightarrow \omega(\rho^0) \pi^+$  is given by

$$\Gamma = \frac{G_f^2 k^3}{8\pi m_1^2} \left| \sum_i \mathcal{A}_i^{(\rho), (\omega)} + \mathcal{B} \right|^2, \quad (A9)$$

with  $M$  the  $D_s$  mass and  $m_{1,2}$  the vector and the pseudoscalar meson masses, respectively, while

$$k = \frac{1}{2M} \{ [M^2 - (m_1 + m_2)^2] [M^2 - (m_1 - m_2)^2] \}^{1/2} \quad (A10)$$

is the size of the three-momentum of the final particles in the  $D_s$  rest frame.

- 
- [1] CLEO Collaboration, R. Balest *et al.*, Phys. Rev. Lett. **79**, 1436 (1997).  
[2] E687 Collaboration, P.L. Frabetti *et al.*, Phys. Lett. B **407**, 79 (1997).  
[3] E791 Collaboration, E.M. Aitala *et al.*, Phys. Rev. Lett. **86**, 765 (2001).  
[4] Particle Data Group, K. Hagiwara *et al.*, Phys. Rev. D **66**, 010001 (2002).  
[5] M. Gourdin, Y.Y. Keum, and X.Y. Pham, Phys. Rev. D **53**, 3687 (1996).  
[6] FOCUS Collaboration, D. Pedrini (private communication).  
[7] M. Bauer, B. Stech, and M. Wirbel, Z. Phys. C **34**, 103 (1987).  
[8] F. Buccella, M. Lusignoli, G. Miele, A. Pugliese, and P. Santorelli, Phys. Rev. D **51**, 3478 (1995).  
[9] F. Buccella, M. Lusignoli, and A. Pugliese, Phys. Lett. B **379**, 249 (1996).  
[10] M. Bando, T. Kugo, S. Uehara, K. Yamawaki, and T. Yanagida, Phys. Rev. Lett. **54**, 1215 (1985); M. Bando, T. Kugo, and K. Yamawaki, Nucl. Phys. B **259**, 493 (1985); Phys. Rep. **164**, 217 (1988).  
[11] T. Fujiwara, T. Kugo, H. Terao, S. Uehara, and K. Yamawaki, Prog. Theor. Phys. **73**, 926 (1985).  
[12] A. Bramon, A. Grau, and G. Pancheri, Phys. Lett. B **344**, 240 (1995).  
[13] T. Feldmann, P. Kroll, and B. Stech, Phys. Rev. D **58**, 114006 (1998); Phys. Lett. B **449**, 339 (1999).  
[14] I. Hinchliffe and T.A. Kaeding, Phys. Rev. D **54**, 914 (1996).  
[15] D. Melikhov and B. Stech, Phys. Rev. D **62**, 014006 (2000).  
[16] D. Becirevic, Nucl. Phys. B (Proc. Suppl.) **94**, 337 (2001); N. Yamada, hep-lat/0210035; S.M. Ryan, Nucl. Phys. B (Proc. Suppl.) **106**, 86 (2002).  
[17] C.W. Chiang, Z. Luo, and J.L. Rosner, Phys. Rev. D **67**, 014001 (2003).